



ORIGINAL ARTICLE

Highly selective and sensitive optosensing of glutathione based on fluorescence resonance energy transfer of upconversion nanoparticles coated with a Rhodamine B derivative



Thu-Thuy T. Nguyen^a, Bui The Huy^{a,b}, Salah M. Tawfik^a, Gerelkhuu Zayakhuu^a,
Hyo Hyun Cho^c, Yong-Ill Lee^{a,*}

^a Department of Chemistry, Changwon National University, Changwon 51140, Republic of Korea

^b Institute of Research and Development, Duy Tan University, 03 Quang Trung, Da Nang, Viet Nam

^c Research Institute, Il-Yang Pharmaceutical Co., Ltd., Yongin 16946, Republic of Korea

Received 20 December 2017; accepted 27 June 2018

Available online 6 July 2018

KEYWORDS

Upconversion;
FRET;
Derivative dye;
Open-ring;
Thiol

Abstract A Glutathione (GSH) optical sensor with high sensitivity and exceptional selectivity was developed using one-step synthesized-upconversion nanoparticles (UCNPs, NaLuF₄:Gd³⁺, Yb³⁺, Er³⁺) in conjunction with a Rhodamine B derivative (RBD). RBD was loaded on the surface of the UCNPs through non-covalent bonding to serve as an energy acceptor, while UCNPs served as energy donors. The sensor based on a coupling fluorescence resonance energy transfer (FRET) process at an excitation of 980 nm wavelength from UCNP to RBD with a ring-opening process of RBD after the addition of GSH. The sensing probe exhibits a remarkable limit of detection (LOD = 50 nM) for GSH through the enhancement of the fluorescence intensity of RBD at 592 nm, together with a concomitant reduction in the green band of the UCNPs. In addition, the sensing mechanism, characterization of UCNPs, and the selectivity of the fluorescence sensor toward GSH were discussed. The proposed sensor was evaluated on real human serum and urine samples and demonstrated as a highly selective and sensitive probe for the detection of GSH.

© 2018 Production and hosting by Elsevier B.V. on behalf of King Saud University. This is an open access article under the CC BY-NC-ND license (<http://creativecommons.org/licenses/by-nc-nd/4.0/>).

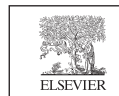
1. Introduction

Thiol compounds play a crucial role in maintaining biological systems. Abnormal levels of cellular thiols have been linked closely to a number of impairments and diseases, including liver damage, cancer, leucocyte loss, neurodegenerative diseases, and AID (Herzenberg et al., 1997, Chen et al., 2010). A decrease in the level of glutathione/glutathione disulfide

* Corresponding author.

E-mail address: yilee@changwon.ac.kr (Y.-I. Lee).

Peer review under responsibility of King Saud University.



Production and hosting by Elsevier

(GSH/GSSG), for example, correlates distinctly to an increased susceptibility to oxidative stress, resulting in pathogenesis and diseases such as Parkinson's and Alzheimer's. It has also been reported that an imbalance in GSH levels accelerates the aging process and presents notable concerns in immune system function (Ballatori et al., 2009; Zaidi and Shin, 2016). N-Acetyl cysteine (NAC), a precursor to glutathione, contributes to its regeneration and is therefore one of our body's most important antioxidants, preventing heart disease, memory loss, and even aging (Koh, 2002). Because thiols significantly affect biological functions at very low levels, it has become a challenge to detect and distinguish between various thiols in biological systems. Therefore, it is essential and urgent to invent a novel method for the detection and discrimination of thiols in health care for effective diagnosis and treatment.

To address these issues, various studies have been conducted to modify and develop different methods to detect specific thiols, such as homocysteine, glutathione, and cysteine. These reported methods include immunoassay separation, capillary electrophoresis, HPLC, and fluorescence approaches (Nekrassova et al., 2003; Li et al., 2009; Chen et al., 2010; Stachniuk et al., 2016). Recently, Rusin reported a colorimetric method for selective detection of Cys and Hcy using unsaturated aldehyde, 3-(4-(dimethylamino) phenyl) acrylaldehyde (Rusin et al., 2004). Additionally, previous studies often relied on UV excitation which has an inherently low light penetration depth and a low signal-to-noise ratio because of the autofluorescence effect (Guan et al., 2016). With respect to the effective fluorescence resonance energy transfer (FRET) process between energy donors and acceptors, the organic-dye-based probes used in previous studies can excite their endogenous chromophores under UV sources, leading to background light interferences, and thus limiting their detections in biomolecules (Zhang et al., 2012). Therefore, it is necessary to develop a novel optosensing probe without background signals that utilize near infrared (NIR) excitation to surmount the above-mentioned challenges.

Upconversion (UC) nanomaterials are smart materials that emit visible wavelengths under excitation of longer NIR wavelengths through a multi-photon process. These materials exhibit low harmfulness of low energy irradiation to analysts, high chemical stability, deep penetrating, non-autofluorescence interference, a high resistance to photo-bleaching and photo-degradation (Chen et al., 2008; Wang et al., 2012; Guan et al., 2016). Among the upconversion materials, host matrices are doped by Yb^{3+} , Er^{3+} ions exhibit strong emissions at green and blue band under an IR excitation. Ni's group presented a nano-platform for Cysteine sensing based on Rhodamine-oxaldehyde functionalized $\text{NaYF}_4:\text{Yb},\text{Er}$ upconversion nanoparticles (UCPs) (Ni et al., 2015). However, their sensor required using cyclodextrine to increase water solubility of UCPs, which were synthesized at high temperature (300 °C using oleic acid), and detection of limit was low ($\sim 1.1 \mu\text{M}$). Recently, Guan's group also reported to use carboxyfluorescein-functionalized UCPs for detecting cysteine with detection of limit $\sim 20 \mu\text{M}$ (Guan et al., 2016). However, they carried out complex process for preparing UCPs. For example, first step- synthesis of $\text{NaYF}_4:\text{Yb},\text{Er}$ core; second step- making a shell NaYF_4 on the $\text{NaYF}_4:\text{Yb},\text{Er}$ core using oleic acid and ODE as solvent; third step- using SiO_2 as a shell for improving water solubility.

Since the green emission from upconversion materials overlaps with the absorption band of RhB, it is expected that these materials could be ideal candidates for FRET optosensing probes (Deng et al., 2011; Yang et al., 2012; Park et al., 2015). In order to develop effective probes for the selective detection of biomolecules, we herein report GSH optosensor based on a coupling FRET process from $\text{NaLuF}_4:\text{Gd}^{3+}, \text{Yb}^{3+}, \text{Er}^{3+}$ UC nanoparticles (UCNPs) to a Rhodamine B derivative (RBD) with the ring - opening process of RBD. Our water solubility UCNPs were synthesized using polyethyleneimine as a surfactant with one-step at low temperature. The ring - opening process occurs through adding GSH. Without GSH, RBD will not emit because the spirocyclic structure of the Rhodamine B is closed by ethylenediamine. The ring opening of RBD helps to visualize the FRET efficiency depending on GSH concentration. This fluorescence behavior is correlated with the spirocyclic structure of the Rhodamine B moiety and the number of conjugated π -bonds in RBD in the presence of GSH. The proposed sensing probe is unique in three following respects: first, the resulting materials with high stability and productivity were obtained through a simple solvothermal synthetic method (200 °C for 12 h); second, the sensing probe exhibited high selectivity and sensitivity toward GSH when compared to other thiols and amino acids; lastly, GSH analysis in human serum and urine samples exhibited the great potential of the developed probe for use in practical applications. Herein, we propose an accessible and economical method to prepare a novel GSH optosensing probe using FRET between UCNPs and RBD, and demonstrate its effective utilization in determination of biomolecules.

2. Experimental

2.1. Chemicals

Gadolinium oxide (Gd_2O_3 99.99%), Ytterbium oxide (Yb_2O_3 99.99%), Lutetium oxide (Lu_2O_3 99.99%), Erbium oxide (Er_2O_3 99.99%), Ammonium fluoride (NH_4F), sodium hydroxide (NaOH), concentrated hydrochloric acid (HCl), methanol (CH_3OH), and polyethyleneimine (PEI, Mw = 25,000) were purchased from Sigma-Aldrich. The ethylene glycol (EG) was obtained from Alfa Aesar. The human serum was supplied by Sigma Chemical Co., and deionized water was used throughout all the experiments. All other chemical reagents in analytical grade were used directly without further purification.

2.2. Preparation of $\text{NaLuF}_4:\text{Gd}^{3+}, \text{Yb}^{3+}, \text{Er}^{3+}$ (UCNPs)

The preparation method for the RECl_3 can be described as follows. Typically, 1 mmol of rare-earth oxides, RE_2O_3 [Lu:Gd:Yb:Er = 68:12:18:2] was dissolved into an HCl solution (2 mL deionized water/1 mL conc. HCl) at 70 °C in a water bath for 3 h. The mixture was evaporated at 60 °C until dryness, and then 2 mL of methanol solution was added to the remaining sample. A solvothermal procedure reported by Zhang was used with some modifications to synthesize PEG-modified, water-soluble $\beta\text{-NaLuF}_4:\text{Gd}^{3+}, \text{Yb}^{3+}, \text{Er}^{3+}$ UCNPs (Zhang et al., 2016). Briefly, NaCl (2.5 mmol), PEI (0.3 g) and 2 mL of RECl_3 solution (1 mmol) were dissolved in ethylene glycol (15 mL) under vigorous stirring. After the solution

became transparent, NH_4F (5 mmol) in 5 mL of EG was dropped slowly to solution under vigorous stirring. The entire resulting mixture was agitated for another 30 min, then transferred to a 40 mL Teflon-lined autoclave and subsequently heated at 200 °C for 12 h. The nanoparticles were collected by centrifugation, washed with ethanol several times, and then dried in a vacuum oven at 50 °C for 24 h.

2.3. Preparation of UCNP@RBD probe

The Rhodamine B derivative (RBD) was synthesized through procedures reported by Zhang and Yu Xiang with some modifications (Xiang et al., 2006; Zhang et al., 2007). Typically, Rhodamine B (1.2 g) was dissolved in EtOH (30 mL). Ethylenediamine (6 mL, excess) was added dropwise to the solution with vigorous stirring and refluxed for 24 h at 90 °C. The obtained solution was light orange in color. After that, the mixture was cooled down, and the solvent was removed under reduced pressure. 50 mL of 0.1 M HCl solution was added dropwise to the solution in the flask to generate a red solution until gas evolution ceased. 30 mL of 1 M NaOH solution was added slowly and stirred until the pH of the solution reached 9 or 10. The resulting precipitation was centrifuged and washed 5 times with water to remove residual starting materials. The final product was kept dry under vacuum at 60 °C for 8 h to obtain a light pink solid in excellent yield (~84%). 50 mg of the prepared UCNPs was mixed with 100 mg of RBD in 10 mL of ethanol solution under stirring for 5 h at room temperature. The RBD-coated UCNPs (UCNP@RBD) were collected by centrifuging and washing with ethanol several times.

2.4. Detection of FRET process between UCNP and RBD

A 100 μL of UCNP@RBD mixture (5 mg of UCNP@RBD in 10 mL of solution ethanol: water (1:10 v/v, phosphate buffered saline, pH = 6–7) was transferred to a cuvette, and then various concentrations of Glutathione were added to the solution. After 10 min of incubation under shaking at room temperature, the fluorescence spectra were recorded within a range from 350 nm to 700 nm using a laser excitation at 980 nm.

2.5. Analysis of glutathione in human serum and urine samples

Analytical samples were prepared on the basis of an easy and fast procedure described as following: The treatment of urine sample was performed according to Jin's group procedure (Jin et al., 2016). Briefly, three samples were collected from different healthy volunteers in the age of 20–55 years old (Changwon, South of Korea) and mixed with acetonitrile (ACN) (ratio of 1:1, v:v) to remove redundant proteins. The mixture was centrifuged at 4000 rpm for 10 min (at 10 °C). The precipitation was discarded, and the upper liquid was diluted 30 times with PBS solution. Human serum (Male) samples were diluted 40-fold with water, enclosed in centrifuge tubes and stored in the refrigerator prior to analyze. The volume of human serum or urine sample was kept constant while different GSH concentrations were varied during the fluorescence spectroscopic measurements. All experiments were performed at room temperature.

2.6. Characterization

The crystallography of the prepared up-conversion nanoparticles was characterized by using D8 advance X-ray diffractometer X'pert Pro MPD (PANalytical, Netherlands) equipped with Cu K α radiation ($\lambda = 0.15406$ nm). A scanning rate of $0.05^\circ \text{ s}^{-1}$ was applied to record the pattern in the 2θ range of 10–80°. The size, morphology and structure of the prepared $\beta\text{-NaLuF}_4\text{:Gd}^{3+}, \text{Yb}^{3+}, \text{Er}^{3+}$ UCP were characterized by a scanning electronic microscopy (SEM) (MIRA-II, Tescan, Czech). The Fourier transform infrared spectroscopy (FT-IR) was performed on a FT/IR-6300 (JASCO, Japan). UV-Vis spectra were obtained using V-670 (JASCO, Japan) with a wavelength range of 190–2700 nm. Fluorescence spectra of UCPs were recorded using FP-6500 (JASCO, Japan) and modified with an external 980 nm laser diode.

3. Results and discussion

3.1. Morphology and structure study

UCNPs were synthesized by employing a solvothermal approach using rare-earth chloride, sodium chloride and ammonium fluoride as precursors at 200 °C. NaLuF_4 was chosen as a host material, Yb^{3+} as a sensitizer and Er^{3+} as an activator. Normally, NaLuF_4 material has two typical phases, hexagonal (β) and cubic (α), and the fluorescence intensity of the hexagonal phase is higher than that of the cubic phase. In this study, Gd^{3+} ions were introduced as doping ions in NaLuF_4 to promote the cubic hexagonal phase transition, ultimately resulting in an increase in up-conversion luminescence intensity (Chen et al., 2008; Wang et al., 2010, 2012). This mechanism is based on the ionic radius of Gd^{3+} being larger than that of Lu^{3+} , resulting in the co-doping of Gd^{3+} ions on NaLuF_4 exhibiting a high tendency towards electron cloud distortion due to an increase in dipole polarizability (Wang et al., 2012; Cui et al., 2014). Additionally, the alteration of the crystal lattice induced by the addition of Gd^{3+} ions is based on the variation of the energy gap between the Stark level of Yb^{3+} ($^2\text{F}_{5/2}$) and Er^{3+} ($^4\text{I}_{11/2}$), subsequently leading to a more effective up-conversion (Klier and Kumke, 2015). Therefore, Gd^{3+} ions were used to promote the cubic-hexagonal phase transition, which was further expected to cause an increase in up-conversion fluorescence intensity. In addition, because UCNPs are composed of three main components including a host matrix, a sensitizer and an activator, Er^{3+} was used as the activator to rearrange the transferred energy from Yb^{3+} and distribute Er^{3+} to its excited energy levels to generate an effective UC emission (Zhou et al., 2015). In terms of the sensitizer position, Yb^{3+} ions are suitable candidates for a UC sensitizer position because Yb^{3+} ions have a trivalent energy level (Chen et al., 2014). However, the dopant concentration of sensitizers significantly affects UC efficiency that is normally kept around 20 mol.% in upconversion nanocrystals, while the concentration of activators is lower than 2 mol.% (Gerelkhuu et al., 2017). In this study, the molar ratio of Lu:Gd:Yb:Er was 68:12:18:2.

The XRD and EDX study investigated the characteristics of the as-prepared $\beta\text{-NaLuF}_4\text{:Gd}^{3+}, \text{Yb}^{3+}, \text{Er}^{3+}$ material. The X-ray diffraction pattern of the prepared UCNPs shows diffraction lines that can be ascribed to $\beta\text{-NaLuF}_4$ structure

(JCPDF No. 27-0726), as shown in Fig. 1a. No peak of any new phases was detected, which indicated the high purity of the prepared product. EDX spectrum confirms the presence of Na, Lu, Yb, F, Gd, and Er in the obtained samples (as shown in Fig. S1). The UCNPs possess a spherical, uniform shape and a narrow size distribution with an average size of 60 nm illustrated in Fig. 1b.

Supplementary data associated with this article can be found, in the online version, at <https://doi.org/10.1016/j.arabjc.2018.06.019>.

As shown in Fig. 1c, the obtained UCNPs produce typical emission bands at 407 nm (blue), 521 nm and 540 nm (green), and 658 nm (red) under an excitation of 980 nm wavelength by a laser source. These bands are assigned to the ${}^2\text{H}_{9/2} \rightarrow {}^4\text{I}_{15/2}$, ${}^2\text{H}_{11/2} \rightarrow {}^4\text{I}_{15/2}$, ${}^4\text{S}_{3/2} \rightarrow {}^4\text{I}_{15/2}$, and ${}^4\text{F}_{9/2} \rightarrow {}^4\text{I}_{15/2}$ transitions of Er^{3+} ions, respectively (Bednarkiewicz et al., 2010; Shan et al., 2010; Wang et al., 2012). The upconversion mechanism can be found in previous reports (Bednarkiewicz et al., 2010; Shan et al., 2010; Zhang et al., 2012; Cui et al., 2014). Until now, the upconversion mechanism can be proposed by an energy transfer upconversion (ETU) and excited-state absorption (ESA) process. In the ETU process, Yb^{3+} ions absorb 980 nm photons due to high absorption cross-section of Yb^{3+} ions

to promote the ${}^2\text{F}_{7/2} \rightarrow {}^2\text{F}_{5/2}$ transition, and then the excited Yb^{3+} ions transfer their energy to neighboring Er^{3+} ions. The ground state of Er^{3+} ion is promoted to the ${}^4\text{I}_{11/2}$ state. In next excitation, another Yb^{3+} ion absorb a second 980 nm photon and transfer its energy to the former excited Er^{3+} ion to result appearance of ${}^4\text{I}_{11/2} \rightarrow {}^4\text{F}_{7/2}$ transition through ESA process. The higher ${}^4\text{G}_{11/2}$ level of Er^{3+} ion is populated through an ESA process of ${}^4\text{S}_{3/2} + \text{photon} \rightarrow {}^4\text{G}_{11/2}$, in which the ${}^4\text{S}_{3/2}$ state is fed non-radiative from the ${}^4\text{F}_{7/2}$ state. The excited Er^{3+} ion relaxes non-radiative to ${}^2\text{H}_{9/2}$, ${}^2\text{H}_{11/2}$, ${}^4\text{S}_{3/2}$ and ${}^4\text{F}_{9/2}$ states. The relaxing process from ${}^2\text{H}_{9/2}$, ${}^2\text{H}_{11/2}$, ${}^4\text{S}_{3/2}$ to ${}^4\text{I}_{15/2}$ state produces a peak of blue emission at 407 nm, and two peaks of green emission at 521 nm, 540 nm. The red emissions at 658 nm are assigned to the ${}^4\text{F}_{9/2} \rightarrow {}^4\text{I}_{15/2}$ transitions of Er^{3+} ions (Fig. 1d).

In the synthetic process, PEI was used as a ligand instead of the conventional SiO_2 encapsulation strategy to minimize the inhibition of FRET efficiency by the SiO_2 layer (Zhang et al., 2007; Deng et al., 2011; Wang et al., 2012). RBD was synthesized from a simple reaction of Rhodamine B and Ethylenediamine in 84% overall yield. The structure of RBD was verified by ${}^1\text{H}$ NMR (200 MHz) analysis (Fig. S2). The ${}^1\text{H}$ NMR spectrum of the as-prepared RBD sample dispersed

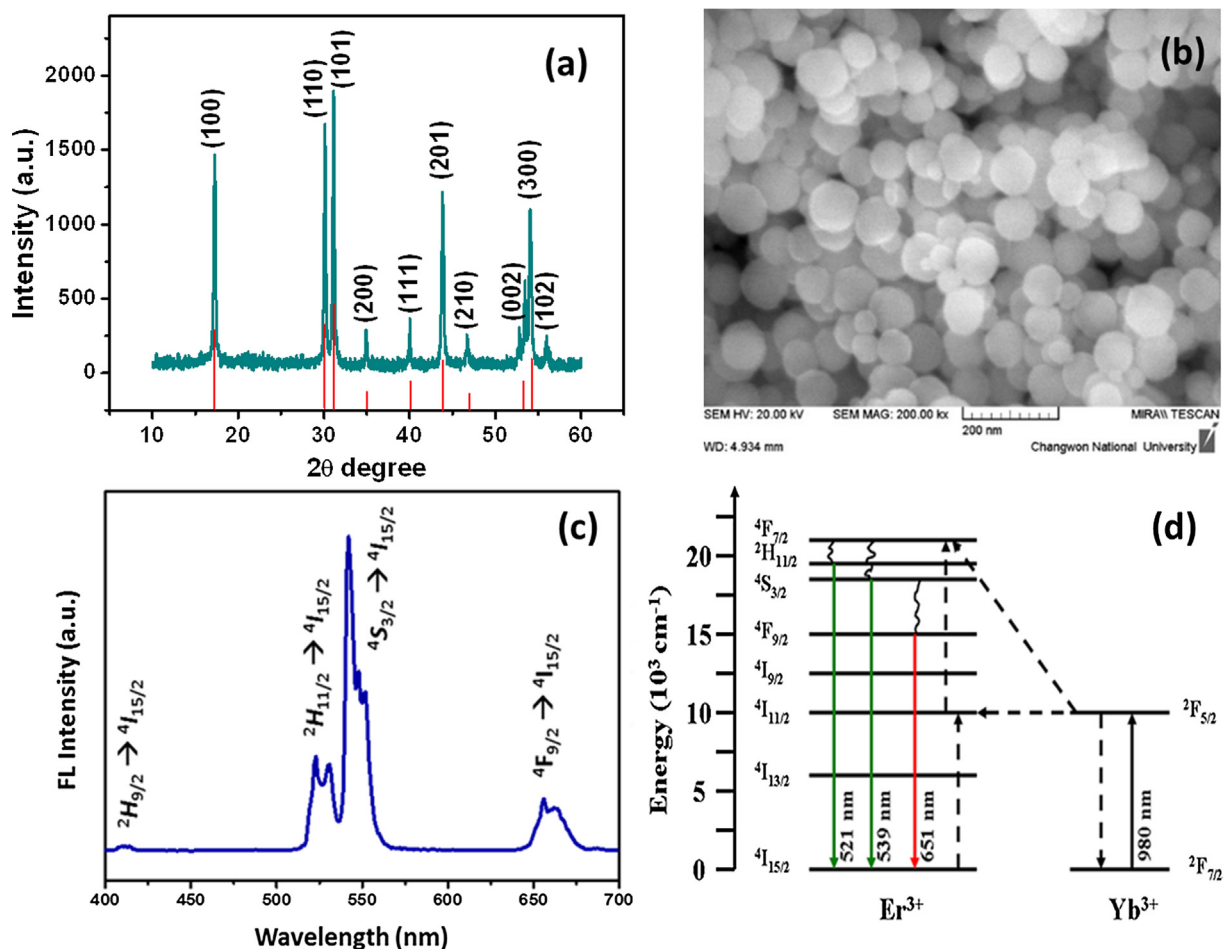


Fig. 1 (a) X-ray diffraction pattern of $\text{NaLuF}_4:\text{Gd}^{3+}, \text{Yb}^{3+}, \text{Er}^{3+}$ (UCNPs) with Miller indexes; (b) SEM image of nanoparticles; (c) fluorescence spectrum of UCNPs under an excitation of 980 nm wavelength; and (d) the proposed upconversion mechanism in $\text{NaLuF}_4:\text{Gd}^{3+}, \text{Yb}^{3+}, \text{Er}^{3+}$ under 980 nm excitation. Solid arrows with different colors indicate the luminescent processes, and the dotted arrows stand for the energy-transfer processes. The multiphotons relaxation processes of Er^{3+} is set as dashed arrows.

in CDCl_3 is consistent with previously reported data for the Rhodamine B derivative, with typical peaks at: δ (ppm) = 10.88 (br, 2H), 7.83–6.22 (m, 10H), 3.66–2.33 (m, 16H), and 1.47–1.13 (12H) (Xiang et al., 2006). The FT-IR spectra of UCP, and UCP@RBD were shown in Fig. S3. The emergence of new stretching vibration peaks in RBD-coated UCNP including 1681, 1614, 1512, 1368, 1219, and 1113 cm^{-1} bands was also considered as an evidence for the successful binding and ligand exchange processes between the amine bonds of UCNP and RBD.

3.2. FRET process between UCNP and RBD

Fig. 2a shows the up-conversion emission spectrum of prepared UCNP under 980 nm excitations and absorption spectrum of the RhB overlap with each other to enable the FRET process. Under an excitation of 980 nm wavelength, dispersed-water UCNP sample exhibited green emission, which can be seen by naked-eye (inset of Fig. 2a). In addition, RBD exhibits a large Stokes shift (Fig. 2b). This also leads to an effective FRET between the UCNP (as the donor) and RBD (as the acceptor). It is interesting to note that the ring-opening is triggered by the addition of GSH. We confirmed that the fluorescent intensity of UCNP did not change with the addition of GSH. Scheme 1 represents a proposed mechanism

of a developed GSH sensor, where the GSH sensing probe was prepared by coating the UCNP with RBD (UCNP@RBD).

The RBD molecules pointed out a non-covalent absorption on the surface of UCNP via hydrophobic interactions. The results show that upon the addition of GSH, the fluorescence emission at 592 nm, which originated from RBD, was immediately enhanced, whereas the green fluorescence emitted by the UCNP was reduced because of fluorescence resonance energy transfer (FRET) from UCNP to RBD, and the red emission band at 658 nm remained unchanged (Fig. 3a). In the presence of GSH, RBD attenuated the green emission of Er^{3+} ions in relation to the unaffected red Er^{3+} emission. RBDs obtained energy from the ${}^2\text{H}_{11/2} + {}^4\text{S}_{3/2} \rightarrow {}^4\text{I}_{15/2}$ transition of Er^{3+} ions in the FRET process, which resulted in the presence of a new yellow emission at 592 nm (Inset of Fig. 3a).

The relationship between the green/red band ratios of UCNP@RBD and GSH concentrations is described by the Stern-Volmer equation:

$$\frac{I_{540}}{I_{658}} = 3.41076 - 0.05[C_{\text{GSH}}]$$

where I_{540} and I_{658} are the fluorescence intensities of green and red emissions from the UCNP, respectively; and $[C_{\text{GSH}}]$ is the concentration of glutathione (μM). The change in the I_{540}/I_{658} or I_{592}/I_{658} ratios was used to determine the GSH

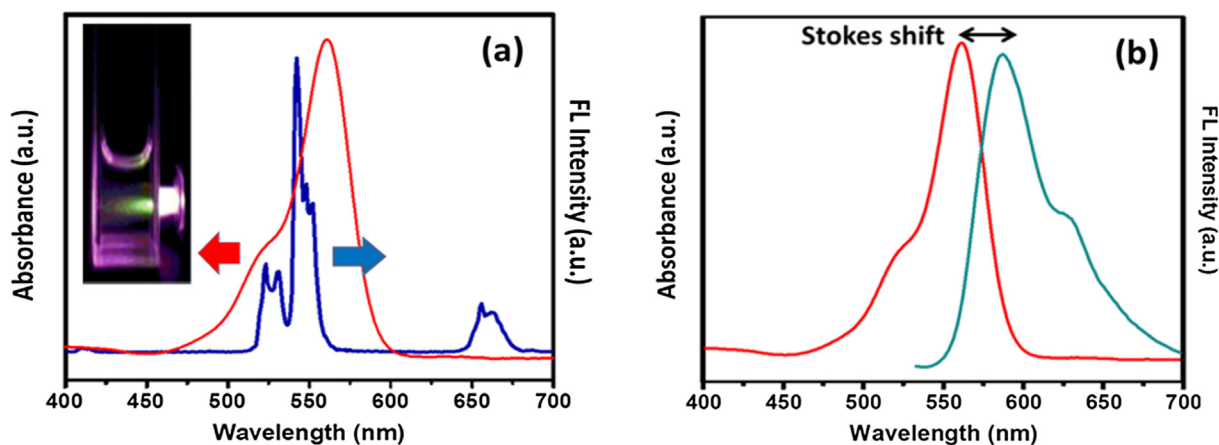
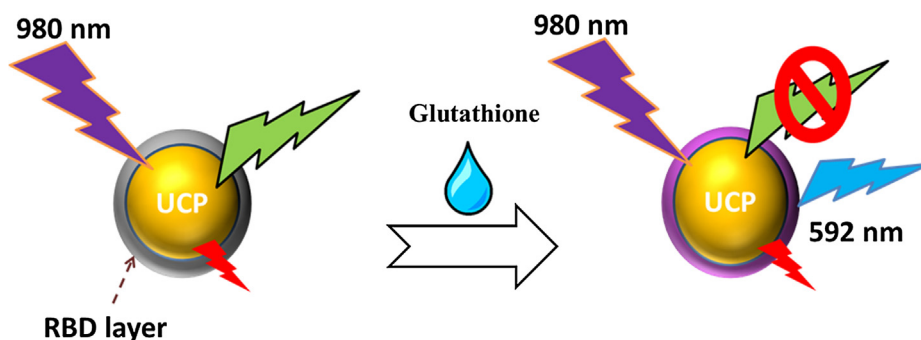


Fig. 2 (a) Fluorescence emission (green line) spectrum ($\lambda_{\text{ex}} = 980$ nm) of UCNP and UV-Vis absorption (red line) spectrum of RBD that overlap each other to make fluorescence resonance energy transfer easy and effective. (Inset: Image of UCNP dispersing in water under 980 nm excitation); (b) The Stokes shift between the absorption and emission spectra of RBD in aqueous solution.



Scheme 1 Proposed mechanism of a developed GSH sensor.

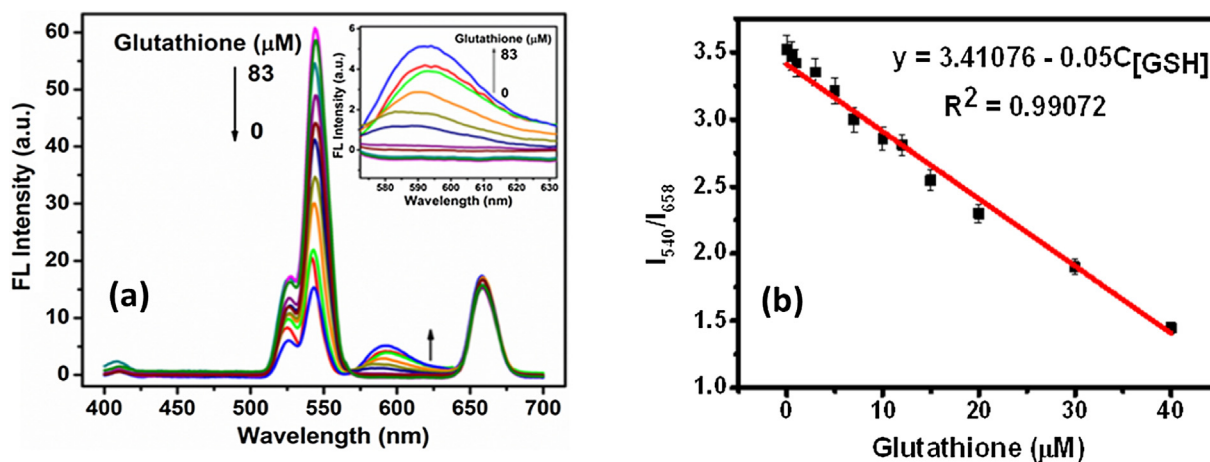


Fig. 3 (a) Fluorescence spectra of UCNP@RBD in the presence of Glutathione (0.3–83 μM) upon 980 nm excitation (Inset: Emission from UCNP@RBD at ~ 592 nm in the presence of GSH), (b) Stern-Volmer-type description of the green ($^2\text{H}_{11/2} + ^4\text{S}_{3/2} \rightarrow ^4\text{I}_{15/2}$) to red ($^4\text{F}_{9/2} \rightarrow ^4\text{I}_{15/2}$) emission ratio (I_{540}/I_{658}), showing linear fit through GSH concentration in the range of 0.3–40 μM upon 980 nm excitation in aqueous solution at room temperature.

concentration (Figs. 3b and S4 Supplementary data). Because the RBD doesn't exhibit any fluorescence emission upon 980 nm excitation, the presence of the new peak at 592 nm of UCNP@RBD confirmed that there is the existence of FRET process between UCNPs and RBD after adding GSH. The response of RBD fluorescence intensity to GSH concentration exhibits a good linear coefficient (R^2) up to 0.99029 and the limit of detection of 0.05 μM was determined to suggest excellent quantification ability.

To evaluate the selectivity of the proposed UCNP@RBD probe, the reactivity of UCNP@RBD toward other thiols was investigated. Upon the addition of other thiol compounds, such as Cysteine (Cys), Mercaptopropionic acid (MPA), and N-acetyl-L-cysteine (NAC), the changes in the fluorescence intensity of UCNP@RBD probes were negligibility despite the fact that the concentrations of other thiols were higher than that of GSH (5 times). Fig. 4a shows the UV-Vis absorption spectra of the prepared UCNP@RBD in the presence of

different thiol groups. The addition of GSH resulted in an increase of absorbance to bring on more effective FRET process. The change of fluorescence intensity could be correlated with the formation of an intermediate complex through the C=O bond (Li et al., 2016).

The proposed aspects of selectivity between thiol compounds are dependent on two factors. First, the pKa values of GSH, Cys, NAC, and MPA are 1.94, 2.05, 3.24, and 4.34, (GSH < Cys < NAC < MPA) respectively. And the high pKa values of the thiol compounds limit their reactivity (Li et al., 2016). Second, both $-\text{SH}$ and $-\text{COOH}$ participate in the reaction with RBD and then open RBD's ring. Steric effects between $-\text{SH}$ and $-\text{COOH}$ groups of GSH are less than those of the other thiol compounds. Therefore, the selectivity of UCNP@RBD could be attributed to the higher pKa values of the other thiol compounds. The effect of interferences was estimated, as displayed in Fig. 4b. The results showed that the fluorescence intensity ratios of I_{540}/I_{658} and I_{592}/I_{658} were

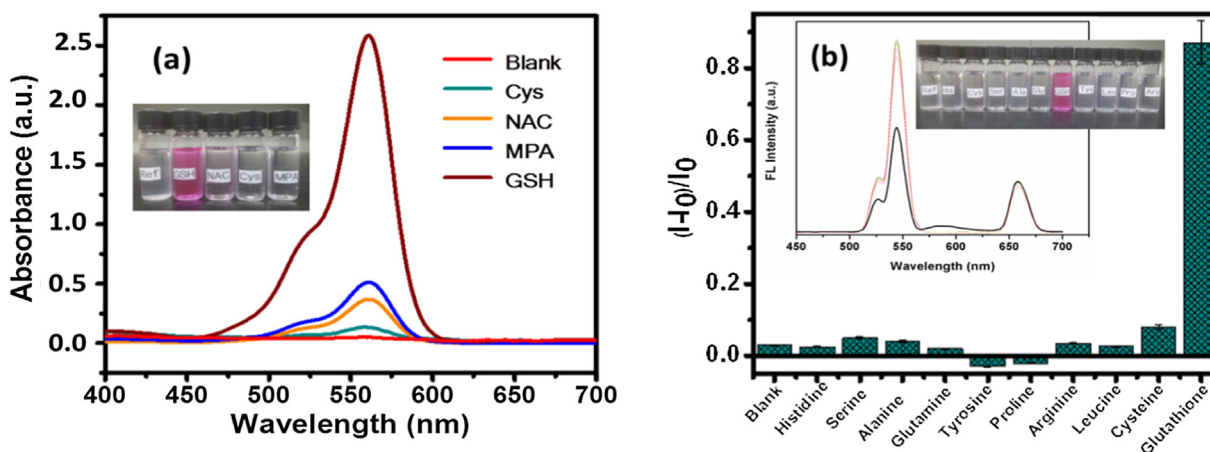


Fig. 4 (a) UV-Vis absorption spectra of the prepared RBD in the presence of various thiol groups (100 μM) and GSH (20 μM) (Inset: Images of probe jars in case of adding GSH (red color), and the other thiols (colorless)). (b) Fluorescence intensity ratios I_{592}/I_{658} of the proposed probe to GSH and different amino acid as interferences. (Inset: FL spectra and images of probe jars – jar with red color (adding GSH), and jars with colorless (adding different amino acids as interferences)).

not obviously changed, except for GSH to demonstrate a high selectivity of UCNP@RBD probe. The color change of the sensing system with the addition of GSH can be directly observed by the naked eyes, as shown in the inset of Fig. 4b.

Based on the obtained results, the mechanism of our GSH sensor is proposed in Scheme 2. The affinity of RBD towards GSH may be related to both the $-\text{COOH}$ and $-\text{SH}$ groups, leading to the ring-opening process of RBD and the recovery of the original colour of Rhodamine B. The GSH-sensing mechanism of this probe is based on the change in spirocyclic structure of the Rhodamine B moiety, including cyclic guanylation of the thiourea moiety and promotion of open-cycle forms (Wu et al., 2007). According to the quantum mechanism, the closed and open-cycle forms can be explained in terms of the variation in the number of conjugated π -bonds in RBD before and after adding GSH to the UCNP@RBD solution (Zielinski and Shalhoub, 1998). In the absence of GSH, these probes exist in the spirocyclic form, i.e. the number of π -conjugations totals nine, which is a non-fluorescence arrangement. In the presence of GSH, the bond at N^* is broken, leading to the creation of one additional π -conjugation to the central rings to restore the inherent π -conjugation of RBD to 10 conjugations in the new compound.

We suggest that the oxygen atom of the carbonyl group and the nitrogen atom on the ethylenediamine moiety cooperatively participate in the binding with GSH. This cooperation induced the ring-opening process of RBD. We found that the fluorescence ring-opening form was the consequence of strong electrostatic interactions between the electronegative parts of the oxygen atom of the carbonyl group in Rhodamine B and the electropositive parts of the ammonium ion in GSH. Additionally, interactions in the form of hydrogen bonds between the amine groups of ethylenediamine in RBD and the thiol group in GSH constitutes another force for selectively attracting GSH to the surface of the UCNP@RBD probe.

Scheme S1 Supplementary data explains in detail the two-photon UC and FRET processes where energy levels of Er^{3+} ions (${}^2\text{H}_{11/2} + {}^4\text{S}_{3/2}$ and ${}^4\text{F}_{9/2}$) are populated through the up-conversion process under a 980 nm excitation. First, Yb^{3+} ions absorb the energy from 980 nm excitation, and then its energy is transferred to surrounding Er^{3+} ions.

Subsequently, the energy from green emission of Er^{3+} ions of the UCNPs transfer to RBD either through photon-reabsorption or FRET, in which the transferred energy corresponds to the valence and conduction bands of RBD (Bednarkiewicz et al., 2010).

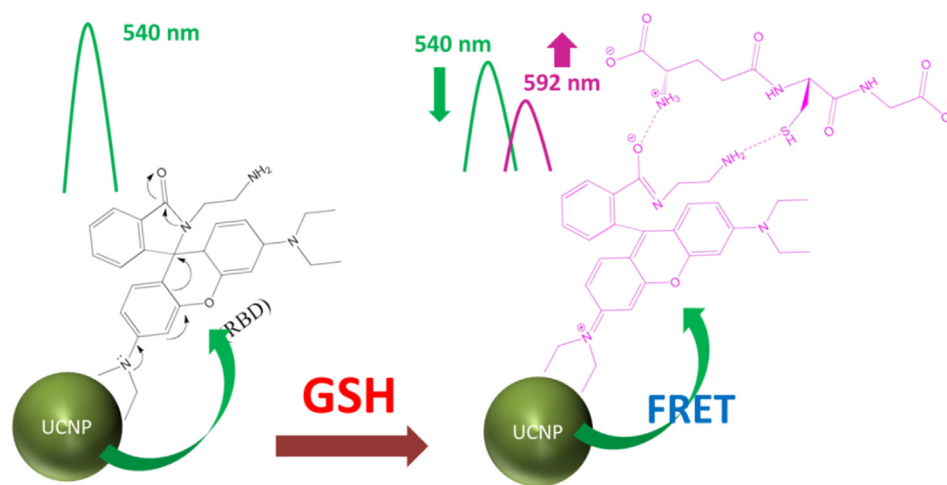
Based on the obtained results, we are convinced that both processes are present in our system where the photon reabsorption is mainly responsible for the I_{540}/I_{658} emission ratio, and the I_{592}/I_{658} emission ratio corresponds to the FRET process. These two processes may originate from the relatively broad overlap area between the emission of the donor and the absorption of the acceptor that is shown in Fig. 2a.

3.3. Detection of glutathione in human serum and urine samples

The analytical reliability and potential application of the proposed probes were evaluated on human serum and urine samples under optimum experimental conditions. Using a spiked technique, the results of the recovery values for detecting GSH using the UCNP@RBD probe in human serum and urine samples are listed in Table 1. The recoveries of GSH in human serum samples ranged from 98.26 to 105.80%, while the recoveries obtained from human urine samples ranged from 95.72 to 103.43%. The obtained RSD values indicate a suitable accuracy of the proposed probes for detecting GSH

Table 1 Spiked recovery results for determination of Glutathione using UCNP@RBD in human serum and urine samples.

Samples	Added GSH (μM)	Detected GSH (μM)	Recovery (%)	RSD (%)
Human serum	30	30.64	102.13	3.06
	70	74.11	105.80	1.76
	120	118.46	98.72	2.51
	170	167.05	98.26	2.08
Urine	20	21.04	101.21	1.61
	70	67.00	95.72	3.16
	120	117.85	98.21	4.44
	170	175.83	103.43	2.03



Scheme 2 FRET between UCNP and RBD after adding GSH under an excitation of 980 nm wavelength. Ring-opened mechanism of RBD in the presence of GSH.

Table 2 A comparison of the proposed probe with previous methods.

Probes	LOD	Linear range	Ref.
CdTe Chemiluminescence	2 nM	2.0 nM–6.5 μ M	Liu et al. (2013a)
g-C ₃ N ₄	20 nM	0.05–900 μ M	Yang et al. (2017)
MnO ₂ -UCP	0.9 μ M		Deng et al. (2011)
GO-CdTe QDs	8.3 μ M	24–214 μ M	Wang et al. (2009)
BSA-MnO ₂ NPs	0.1 μ M	0.26–26 μ M	Liu et al. (2013b)
CdSe/ZnS/Nafion films	1.5 μ M	10.1–200 μ M	Dennany et al. (2011)
Citidine-modified Au	20 nM	20 nM–3 μ M	Jiang et al. (2016)
Hierarchical Ag	4.11 μ M		Sanskriti and Upadhyay (2017)
Au NPs	0.5 μ M	0.5–1.25 μ M	Hu et al. (2013)
Enzyme-mimetic Co ₃ O ₄	33 nM	0.5–10 μ M	Wang et al. (2016)
Graphen QDs	43 nM	0.2–85 μ M	Liu et al. (2016)
UCNP@RBD	50 nM	0.3–40 μ M	This work

in biological samples. All experiments were conducted with five measurements.

To evaluate the competition and the efficiency of the proposed probe with previous methods, Table 2 displays a comparison in the LOD and linear range values. In terms of effectiveness and reliability, this proposed method takes advantage of a very low detection, and high selectivity for GSH detection, in comparison with others previously reported.

The pH dependence of proposed sensor was estimated. The results showed that FL intensity of UCP@RBD didn't change in range of 4–10. Besides, the stability of UCP@RBD in term of time was estimated at room temperature. The results demonstrated the prepared UCP@RBD probe was stable within 60 days, as shown in Fig. S5.

4. Conclusions

We have developed a simple GSH sensing probe that relies on the ring-opening process of RBD and the FRET process between UCNPs and RBD with a remarkable analytical performance. The GSH sensing probe effectively integrates two essential features: high selectivity towards GSH and no luminescence background. This approach eliminates both autofluorescence of biological samples and background signals. Additionally, the use of the ring-opening process of RBD and the FRET between UCNPs and RBD enabled us to propose a very simple approach for making GSH probe. The proposed UCP@RBD probe exhibited excellent selectivity and high sensitivity. We also demonstrated the high reliability and efficiency of probe to detect GSH in human serum and urine samples. These results suggest that this simple concept of UCP-coupled sensors for the highly selective and sensitive detection of biological entities enables expansion into various biological applications.

Acknowledgments

This research was supported by Basic Science Research Program through the National Research Foundation of Korea (NRF) funded by the Ministry of Education (NRF-2017R1D1A3B03035530 and NRF-2017R1A2B4006388) and the Creative Fusion R&D for Regional Industry Program operated by the Ministry of Trade, Industry and Energy (No. R0005386).

References

- Ballatori, N., Krance, S.M., Notenboom, S., Shi, S., Tieu, K., Hammond, C.L., 2009. Glutathione dysregulation and the etiology and progression of human diseases. *Biol. Chem.* 390 (3), 191–214.
- Bednarkiewicz, A., Nyk, M., Samoc, M., Strek, W., 2010. Up-conversion FRET from Er³⁺/Yb³⁺:NaYF₄ Nanophosphor to CdSe Quantum Dots. *J. Phys. Chem. C* 114 (41), 17535–17541.
- Chen, G., Qiu, H., Prasad, P.N., Chen, X., 2014. Upconversion nanoparticles: design, nanochemistry, and applications in theranostics. *Chem. Rev. (Washington, DC, U. S.)* 114 (10), 5161–5214.
- Chen, X., Zhou, Y., Peng, X., Yoon, J., 2010. Fluorescent and colorimetric probes for detection of thiols. *Chem. Soc. Rev.* 39 (6), 2120–2135.
- Chen, Z., Chen, H., Hu, H., Yu, M., Li, F., Zhang, Q., Zhou, Z., Yi, T., Huang, C., 2008. Versatile synthesis strategy for carboxylic acid-functionalized upconverting nanophosphors as biological labels. *J. Am. Chem. Soc.* 130 (10), 3023–3029.
- Cui, Y., Zhao, S., Liang, Z., Han, M., Xu, Z., 2014. Optimized upconversion emission of NaLuF₄:Er, Yb nanocrystals codoped with G^{d3+} ions and its mechanism. *J. Alloys Compd.* 593, 30–33.
- Deng, R., Xie, X., Vendrell, M., Chang, Y.-T., Liu, X., 2011. Intracellular glutathione detection using MnO₂-nanosheet-modified upconversion nanoparticles. *J. Am. Chem. Soc.* 133 (50), 20168–20171.
- Dennany, L., Gerlach, M., O'Carroll, S., Keyes, T.E., Forster, R.J., Bertonecello, P., 2011. Electrochemiluminescence (ECL) sensing properties of water soluble core-shell CdSe/ZnS quantum dots/Nafion composite films. *J. Mater. Chem.* 21 (36), 13984–13990.
- Gerekhuu, Z., Huy, B.T., Chung, J.W., Phan, T.-L., Conte, E., Lee, Y.-I., 2017. Influence of Cr³⁺ on upconversion luminescent and magnetic properties of NaLu_{0.86-x}Gd_{0.12}F₄:Cr³⁺/Er³⁺ (0 ≤ x ≤ 0.24) material. *J. Lumin.* 187, 40–45.
- Guan, Y., Qu, S., Li, B., Zhang, L., Ma, H., Zhang, L., 2016. Ratiometric fluorescent nanosensors for selective detecting cysteine with upconversion luminescence. *Biosens. Bioelectron.* 77, 124–130.
- Herzenberg, L.A., De Rosa, S.C., Dubs, J.G., Roederer, M., Anderson, M.T., Ela, S.W., Deresinski, S.C., Herzenberg, L.A., 1997. Glutathione deficiency is associated with impaired survival in HIV disease. *Proc. Natl. Acad. Sci. USA* 94 (5), 1967–1972.
- Hu, B., Cao, X., Zhang, P., 2013. Selective colorimetric detection of glutathione based on quasi-stable gold nanoparticles assembly. *New J. Chem.* 37 (12), 3853–3856.
- Jiang, H., Su, X., Zhang, Y., Zhou, J., Fang, D., Wang, X., 2016. Unexpected thiols triggering photoluminescent enhancement of cytidine stabilized Au nanoclusters for sensitive assays of glutathione reductase and its inhibitors screening. *Anal. Chem.* 88 (9), 4766–4771.

- Jin, D., Seo, M.-H., Huy, B.T., Pham, Q.-T., Conte, M.L., Thangadurai, D., Lee, Y.-I., 2016. Quantitative determination of uric acid using CdTe nanoparticles as fluorescence probes. *Biosens. Bioelectron.* 77, 359–365.
- Klier, D.T., Kumke, M.U., 2015. Upconversion NaYF₄:Yb: Er nanoparticles co-doped with G^{d3+} and N^{d3+} for thermometry on the nanoscale. *RSC Adv.* 5 (82), 67149–67156.
- Koh, A.S., 2002. Identification of a mechanism by which the methylmercury antidotes N-acetylcysteine and dimercaptopropane-sulfonate enhance urinary metal excretion: transport by the renal organic anion transporter. *Mol. Pharmacol.* 62 (4), 921–926.
- Li, D.-P., Zhang, J.-F., Cui, J., Ma, X.-F., Liu, J.-T., Miao, J.-Y., Zhao, B.-X., 2016. A ratiometric fluorescent probe for fast detection of hydrogen sulfide and recognition of biological thiols. *Sens. Actuators, B* 234, 231–238.
- Li, H., Fan, J., Wang, J., Tian, M., Du, J., Sun, S., Sun, P., Peng, X., 2009. A fluorescent chemodosimeter specific for cysteine: effective discrimination of cysteine from homocysteine. *Chem. Commun.* (39), 5904–5906.
- Liu, L., Ma, Q., Li, Y., Liu, Z., Su, X., 2013a. Detection of biothiols in human serum by QDs based flow injection “turn off-on” chemiluminescence analysis system. *Talanta* 114, 243–247.
- Liu, X., Wang, Q., Zhang, Y., Zhang, L., Su, Y., Lv, Y., 2013b. Colorimetric detection of glutathione in human blood serum based on the reduction of oxidized TMB. *New J. Chem.* 37 (7), 2174–2178.
- Liu, Z., Gong, Y., Fan, Z., 2016. A dopamine-modulated nitrogen-doped graphene quantum dot fluorescence sensor for the detection of glutathione in biological samples. *New J. Chem.* 40 (10), 8911–8917.
- Nekrassova, O., Lawrence, N.S., Compton, R.G., 2003. Analytical determination of homocysteine: a review. *Talanta* 60 (6), 1085–1095.
- Ni, J., Shan, C., Li, B., Zhang, L., Ma, H., Luo, Y., Song, H., 2015. Assembling of a functional cyclodextrin-decorated upconversion luminescence nanoplatform for cysteine-sensing. *Chem. Commun.* 51 (74), 14054–14056.
- Park, Y.I., Lee, K.T., Suh, Y.D., Hyeon, T., 2015. Upconverting nanoparticles: a versatile platform for wide-field two-photon microscopy and multi-modal in vivo imaging. *Chem. Soc. Rev.* 44 (6), 1302–1317.
- Rusin, O., St. Luce, N.N., Agbaria, R.A., Escobedo, J.O., Jiang, S., Warner, I.M., Dawan, F.B., Lian, K., Strongin, R.M., 2004. Visual detection of cysteine and homocysteine. *J. Am. Chem. Soc.* 126 (2), 438–439.
- Sanskriti, I., Upadhyay, K.K., 2017. Cysteine, homocysteine and glutathione guided hierarchical self-assemblies of spherical silver nanoparticles paving the way for their naked eye discrimination in human serum. *New J. Chem.* 41 (11), 4316–4321.
- Shan, J., Uddi, M., Wei, R., Yao, N., Ju, Y., 2010. The hidden effects of particle shape and criteria for evaluating the upconversion luminescence of the lanthanide doped nanophosphors. *J. Phys. Chem. C* 114 (6), 2452–2461.
- Stachniuk, J., Kubalczyk, P., Furmaniak, P., Głowacki, R., 2016. A versatile method for analysis of saliva, plasma and urine for total thiols using HPLC with UV detection. *Talanta* 155, 70–77.
- Wang, F., Han, Y., Lim, C.S., Lu, Y., Wang, J., Xu, J., Chen, H., Zhang, C., Hong, M., Liu, X., 2010. Simultaneous phase and size control of upconversion nanocrystals through lanthanide doping. *Nature* 463 (7284), 1061–1065.
- Wang, T., Su, P., Li, H., Yang, Y., Yang, Y., 2016. Triple-enzyme mimetic activity of Co₃O₄ nanotubes and their applications in colorimetric sensing of glutathione. *New J. Chem.* 40 (12), 10056–10063.
- Wang, Y., Lu, J., Tang, L., Chang, H., Li, J., 2009. Graphene oxide amplified electrogenerated chemiluminescence of quantum dots and its selective sensing for glutathione from thiol-containing compounds. *Anal. Chem.* 81 (23), 9710–9715.
- Wang, Y., Shen, P., Li, C., Wang, Y., Liu, Z., 2012. Upconversion fluorescence resonance energy transfer based biosensor for ultra-sensitive detection of matrix metalloproteinase-2 in blood. *Anal. Chem.* 84 (3), 1466–1473.
- Wu, J.-S., Hwang, I.-C., Kim, K.S., Kim, J.S., 2007. Rhodamine-based Hg²⁺-selective chemodosimeter in aqueous solution: fluorescent OFF–ON. *Org. Lett.* 9 (5), 907–910.
- Xiang, Y., Tong, A., Jin, P., Ju, Y., 2006. New fluorescent rhodamine hydrazone chemosensor for Cu(II) with high selectivity and sensitivity. *Org. Lett.* 8 (13), 2863–2866.
- Yang, C., Wang, X., Liu, H., Ge, S., Yu, J., Yan, M., 2017. On-off-on fluorescence sensing of glutathione in food samples based on a graphitic carbon nitride (g-C₃N₄)-Cu²⁺ strategy. *New J. Chem.* 41 (9), 3374–3379.
- Yang, T., Sun, Y., Liu, Q., Feng, W., Yang, P., Li, F., 2012. Cubic sub-20 nm NaLuF₄-based upconversion nanophosphors for high-contrast bioimaging in different animal species. *Biomaterials* 33 (14), 3733–3742.
- Zaidi, S.A., Shin, J.H., 2016. A review on the latest developments in nanostructure-based electrochemical sensors for glutathione. *Anal. Methods* 8 (8), 1745–1754.
- Zhang, J., Li, B., Zhang, L., Jiang, H., 2012. An optical sensor for Cu (II) detection with upconverting luminescent nanoparticles as an excitation source. *Chem. Commun.* 48 (40), 4860–4862.
- Zhang, X., Shiraishi, Y., Hirai, T., 2007. Cu(II)-selective green fluorescence of a rhodamine–diacetic acid conjugate. *Org. Lett.* 9 (24), 5039–5042.
- Zhang, Z., Zhang, M., Wu, X.-Y., Chang, Z., Lee, Y.-I., Huy, B.T., Sakthivel, K., Liu, J.-F., Jiang, G.-B., 2016. Upconversion fluorescence resonance energy transfer—a novel approach for sensitive detection of fluoroquinolones in water samples. *Microchem. J.* 124, 181–187.
- Zhou, J., Liu, Q., Feng, W., Sun, Y., Li, F., 2015. Upconversion luminescent materials: advances and applications. *Chem. Rev.* (Washington, DC, U. S.) 115 (1), 395–465.
- Zielinski, T.J., Shalhoub, G.M., 1998. Vibronic spectra of diatomic molecules and the birge-spencer extrapolation: BirgeSpencer.mcd. *J. Chem. Educ.* 75 (9), 1192.